ACS APPLIED MATERIALS & INTERFACES

Research Article

www.acsami.org

Bending Induced Self-Organized Switchable Gratings on Polymeric Substrates

Julian Parra-Barranco,[†] Manuel Oliva-Ramirez,[†] Lola Gonzalez-Garcia,[†] Maria Alcaire,[†] Manuel Macias-Montero,[†] Ana Borras,[†] Fabian Frutos,[‡] Agustin R. Gonzalez-Elipe,[†] and Angel Barranco*[,†]

[†]Nanotechnology on Surfaces Laboratory, Instituto de Ciencia de Materiales de Sevilla, Consejo Superior de Investigaciones Científicas (CSIC)-Universidad de Sevilla. c/Américo Vespucio 49, Sevilla 41092, ES, Spain

[‡]Dept. Física Aplicada, ETSII, Universidad de Sevilla, Avda. Reina Mercedes s/n, Sevilla 41012, ES, Spain

Supporting Information

ABSTRACT: We present a straightforward procedure of self-surface patterning with potential applications as large area gratings, invisible labeling, optomechanical transducers, or smart windows. The methodology is based in the formation of parallel micrometric crack patterns when polydimethylsiloxane foils coated with tilted nanocolumnar SiO_2 thin films are manually bent. The SiO_2 thin films are grown by glancing angle deposition at room temperature. The results indicate that crack spacing is controlled by the film nanostructure independently of the film thickness and bending curvature. They also show that the in-plane microstructural anisotropy of the SiO_2 films due to column association perpendicular to the growth direction determines the anisotropic formation of parallel cracks along two main axes. These self-organized patterned foils are completely transparent and work as customized reversible diffraction gratings under mechanical activation.

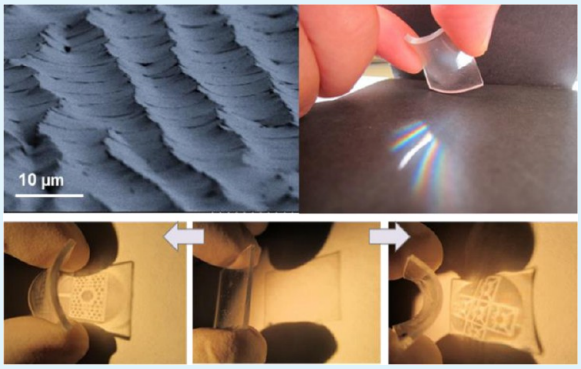

KEYWORDS: *bending, switchable gratings, flexible polymers, polydimethylsiloxane, PDMS, SiO_2 thin films, TiO_2 thin films, GLAD, oblique angle deposition, functional thin films*

1. INTRODUCTION

After prolonged immersion in water the skin expands, producing the universally experienced pruney fingers. Similar surface instabilities are ubiquitous in nature and arise whenever a stiff film coats a compliant substrate. The field of surface instabilities in engineered thin films is in continuous expansion since the pioneering publications by Whiteshides and co-workers on hierarchical surface patterning[1−3] inspired a rich variety of applications such as optical gratings,[2] nanofluidic manipulation,[4−6] controlled cell adhesion surfaces,[7] and others.[8,9] In addition, surface wrinkling is the basis of novel successful methodologies of thin film and coating properties characterization.[10−13]

Glancing angle deposition (GLAD) of evaporated layers is a well-established methodology for the fabrication of tilted oriented nanocolumnar thin films.[14−17] By this method the substrate surface is placed at a glancing angle with respect to the evaporation source, and this particular film microstructure is the result of shadowing effects during the film growth produced by the arriving of a vapor flux at a glancing angle ($\theta \geq 60°$) with respect to the substrate surface.[14] In some materials like SiO_2, the tilted nanocolumns tend to aggregate along a direction perpendicular to the incoming vapor flux forming strongly anisotropic surfaces.[18] This process known as bundling[19] has been recently utilized for the fabrication of tunable dichroic optical structures.[20,21]

Herein we studied the process of self-structuring of transparent SiO_2 GLAD films deposited on polydimethylsiloxane (PDMS) when subjected to manual bending. The results demonstrate that the properties of the patterns generated by this extremely simple process are directly determined by the film nanostructure. Moreover, it is shown that the characteristics of this process differ from those reported for wrinkled surface structures and crack patterns generated on PDMS by combining deposition/surface oxidation and uniaxial strains.[1−9] A thorough characterization of the system microstructure and its phenomenological optical behavior sustain the ample possibilities opened by the proposed methodology for the fabrication of foldable optical devices.

Received: October 31, 2013
Accepted: July 9, 2014
Published: July 9, 2014

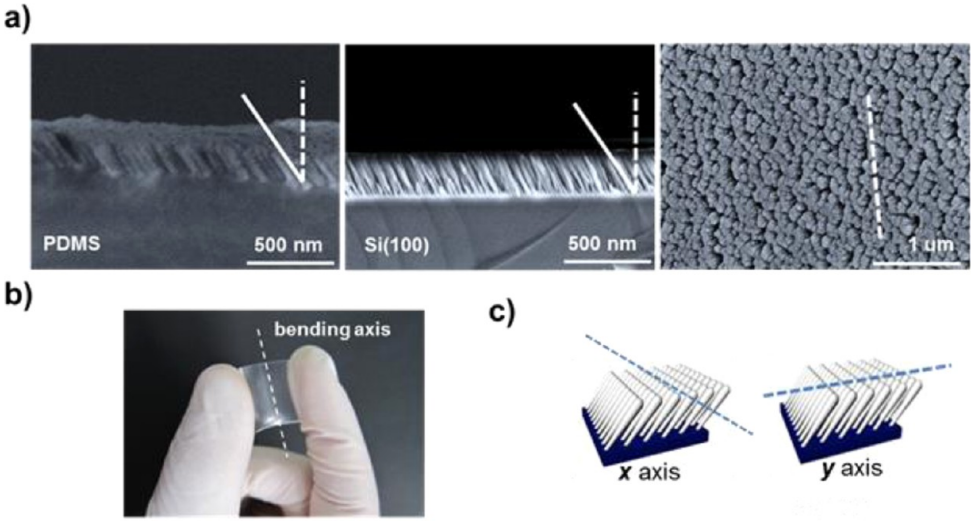

Figure 1. Examples of tilted columnar G-SiO_2 films prepared by GLAD at 80° glancing incidence. (a) Left and center: cross-sectional FESEM micrograph of films deposited on PDMS foil and Si(100); right: FESEM planar view of the latter film showing the preferential column association or bundling along the direction marked by the dash line. The thicknesses of the films in the figures are ~250 nm. (b) Picture showing the procedure required for structuring the surface of a PDMS foil coated with a G-SiO_2 thin film by simply bending the foil after deposition. (c) The schemes show the two axes used for bending as defined with respect to the thin-film anisotropic structure by taking the *x* axis along the nanocolumnar bundling direction.

2. EXPERIMENTAL SECTION

SiO_2 and TiO_2 GLAD thin films were prepared by electron evaporation as reported elsewhere[21−23] at the glancing angles of θ = 60°, 70°, 80°, and 85°. SiO_2 and TiO pellets were used as targets for the depositions of SiO_2 and TiO_2 thin films, respectively. The evaporations were carried out at a pressure of 10^{-4} Torr of oxygen to obtain stoichiometric films. A calibrated quartz crystal monitor was used to control the individual layer thicknesses for each type of film. The temperature of the sample holder during the deposition of the SiO_2 film was measured to be only 2−4° higher than room temperature. In the case of TiO_2 a water cooled sample holder was used to prevent sample heating during deposition. PDMS foils and Si(100) were used as substrates, the latter for the control of the evaporation process and thin film characteristics. The nanocolumnar films were studied without any additional treatment after deposition.

The PDMS foils with a thickness of 1.5 mm were prepared by mixing the Sylgard 184 (DOW) two-part silicon elastomer and degassing and curing the mixture at 80 °C during 30 min. After this process, the foils were cut in pieces of 2 × 2 cm^2.

Field emission scanning electron microscopy (FESEM) characterization was carried out with a Hitachi S4800 microscope. Planar views of thin films on Si(100) and PDMS were measured as deposited. The cross sections of films on PDMS were measured after coating the films with a thin gold layer to reduce charging effects during the characterization.

The UV−vis transmission of the films was measured with a Cary 100 spectrophotometer from Varian. Diffracted light pattern intensities were measured with a calibrated visible-light photometer PMMA2100 from Solar Light Co.

The curvature (κ) of the coated foils during the diffraction measurements is taken as the inverse of the radius of the circle that most closely approximates the curve in the position of the bending axis illuminated with the laser. The values were calculated from pictures of the bent film sections in the sample holder during the measurements.

3. RESULTS AND DISCUSSION

3.1. Bending Induced Formation of Parallel Grooves.

In general, cracking of thin films is synonymous with irreversible damage, delamination, and/or device failure. Nevertheless, under certain well-controlled conditions, a tensile stress applied to a film supported on a compliant substrate can induce the development of a regular pattern perpendicular to the resulting strain.[24,25] For example, patterns of cracks produced by uniaxial straining of plasma surface oxidized PDMS foils have been used for the fabrication of protein matrices[26] and nanofluidic channels.[27]

A simpler way of applying stress to a PDMS foil is by bending. We have found that when this elastomeric polymer coated with a relatively rigid silicon dioxide layer is bent, irregular cracks are formed to release the accumulated mechanical stress. Figure S1a−c in the Supporting Information shows a series of micrographs of PDMS foils bent after being coated with continuous SiO_2 thin films. These experiments have been conducted with SiO_2/PDMS systems fabricated by surface oxidation with an oxygen plasma[28] (cf. Supporting Information, Figure S1a), plasma-enhanced chemical vapor deposition[29] (cf. Supporting Information, Figure S1b), or electron evaporation of silica at normal incidence (cf. Supporting Information, Figure S1c), respectively. In the three cases, the slight bending of the coated foils produce the formation of a series of irregular cracks whose number irreversibly increases with additional bending operations. This accumulated cracking is neither controllable nor reproducible and typically yields local delamination after a small number of bending events. As will be shown, bending a PDMS foil coated with a nanocolumnar SiO_2 thin film prepared by physical vapor deposition at glancing angles renders quite different results.

The room-temperature GLAD deposition of SiO_2 on PDMS foils (hereafter called G-SiO_2/PDMS) yields anisotropic nanostructured thin films characterized by a tilted columnar microstructure as shown in Figure 1a. The figure shows an example of the SEM images of a film deposited simultaneously on Si(100) and PDMS foil substrates. Apart from the charge effects that render difficult the observation of films on dielectric substrates such as PDMS by FESEM, the images demonstrate a similar nanocolumnar tilted arrangement in both cases. The determined tilted angles of the nanocolumns are ~55° ± 2° and ~53° ± 2° for the film deposited on Si(100) and PDMS, respectively. Thus, it can be concluded that the PDMS

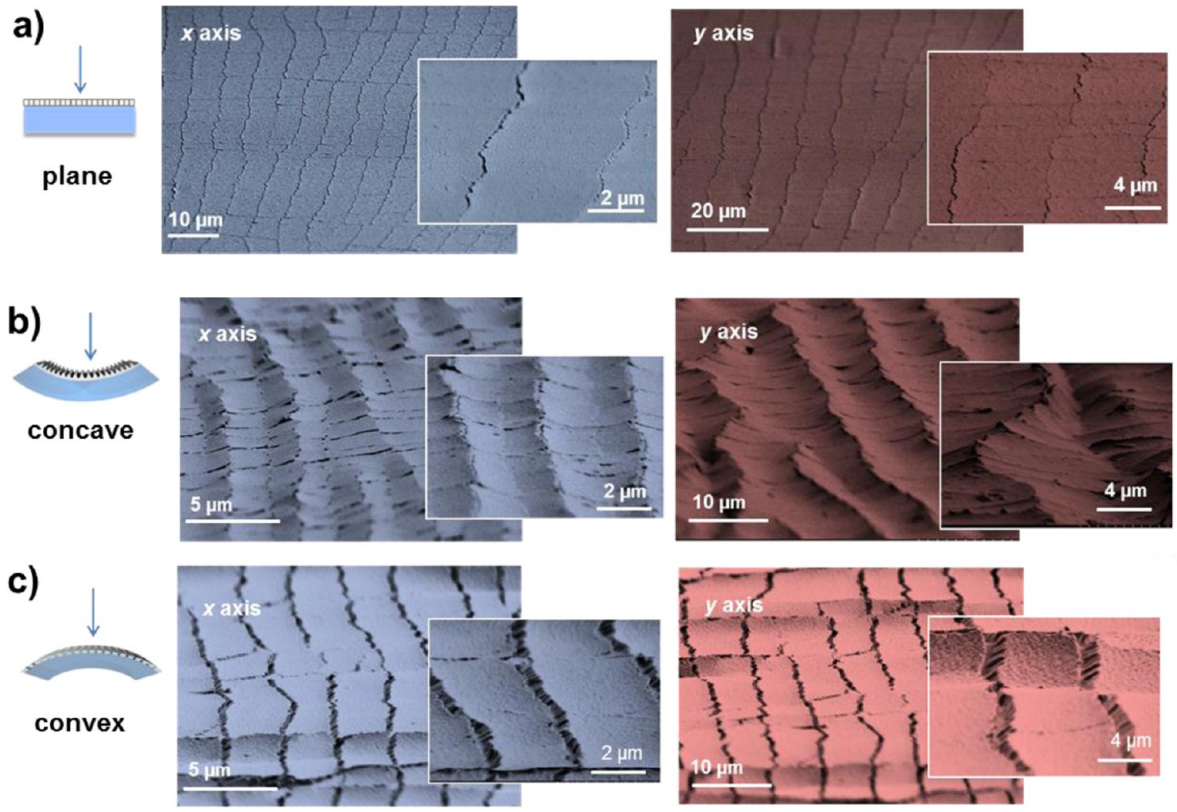

Figure 2. (a) FESEM micrographs of two G-SiO_2/PDMS flat surfaces after bending the coated foils along the *x* (left) and *y* (right) directions. (b) FESEM micrographs of the films in (a) while forming a concave surface during observation. (c) FESEM micrographs of the films in (a) while forming a convex surface during observation. The pictures and graphs in this figure correspond to ~300 nm thick G-85°-SiO_2 films.

substrate does not modify the properties of the glancing angle SiO_2 nanocolumnar thin films. It is known that the nanocolumns tilting angle and porosity of oxide thin films deposited by GLAD increase gradually with the deposition angle, while simultaneously, the number of nanocolumns per unit area decreases.[17,23] Another characteristic microstructural effect sometimes encountered in this type of thin film is the preferential association of the nanocolumns in a direction perpendicular to the arrival flux of material.[19−21] This association is usually designed with the term bundling, and it is known to enhance the surface anisotropy of the system. Clearly, in the G-SiO_2 thin film such bundling association of nanocolumns (see the example in Figure 1a) originates a strong film in-plane anisotropy.[17,19]

As shown in Figure 1b, after thin-film deposition, the G-SiO_2/PDMS foils were manually bent at curvatures of $\kappa \ll 0.55$ cm^{-1} along the orthogonal *y* and *x* axes defined by the nanocolumnar growth and bundling directions, respectively (see Figure 1c).

Figure 2a shows that bending along the *x* axis a G85°-SiO_2/PDMS foil renders a set of parallel and homogeneously separated grooves that, from edge to edge, cover the whole film surface. These grooves, spaced by ~4 μm, result from a regular cracking of the deposited oxide and define a regular pattern parallel to the bending axis. This pattern remains unaltered after actuation on the film for more than 1000 times (as shown below). Bending the same foil along the *y* axis yields a similar pattern with an inter groove spacing of ~6 μm.

A set of G-SiO_2/PDMS foils with different oxide thicknesses were prepared at different glancing angles of deposition to elucidate the relationship between thin-film microstructure and surface patterning upon bending (see examples in Supporting Information, Figure S2). Figure 3 shows the experimental

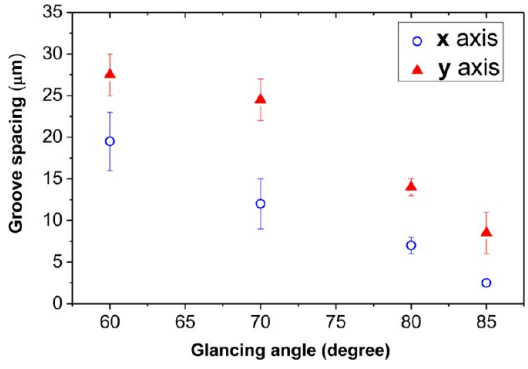

Figure 3. Relationship between the experimental groove spacing values and the thin-film nanostructure determined by the evaporation glancing angle for PDMS covered specimen bent along the *x* and *y* axes.

relationship between the groove spacing and the glancing angle of deposition by bending along the *x* and *y* axes. The groove spacing decreases linearly as the deposition angle increases, being the values corresponding to the *y* axis always higher than those corresponding to the *x* axis. Thus, a first conclusion of this analysis is that the intergroove spacing can be greatly varied by just changing the deposition angle of the G-SiO_2 films. Apart from this relationship between nanocolumnar structure and groove spacing, the experimental results also show that neither the film thickness nor the bending curvature had any

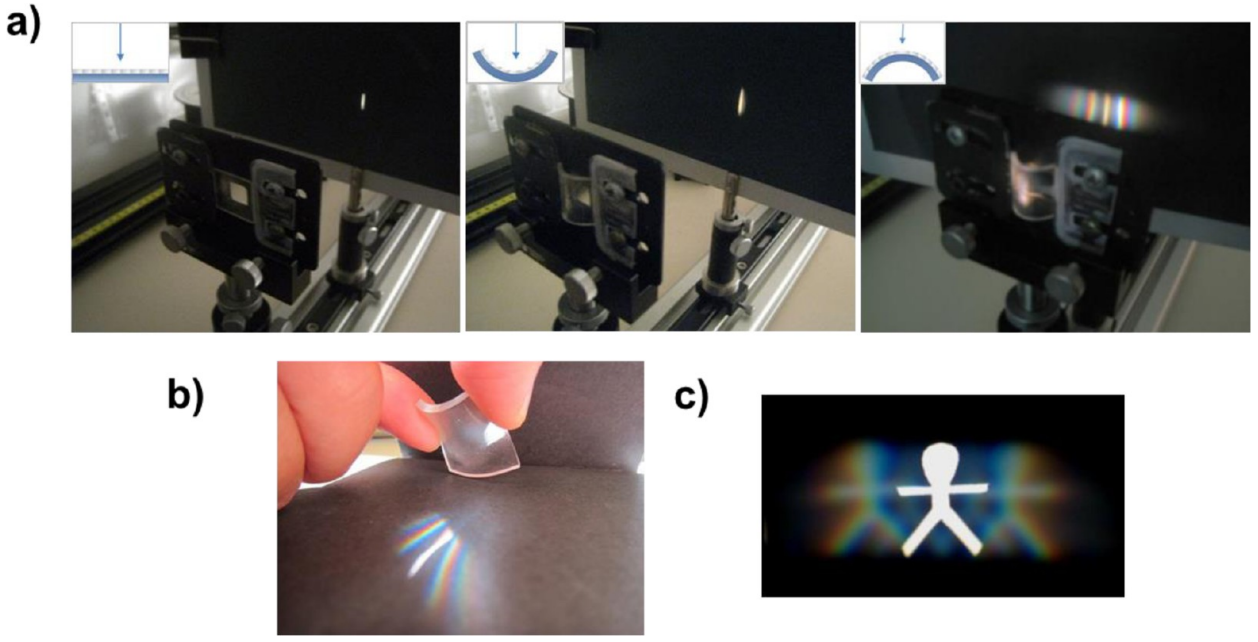

Figure 4. (a) Pictures of a white light beam passing through a G-SiO_2/PDMS foil with a regular groove pattern formed by bending. The light passing through this foil in a flat (left) and convex (center) configuration reaches the screen undisturbed. The light passing through the concave covered surface (right) is diffracted and forms a characteristic rainbow pattern onto the screen. (b) Picture of a concave G-SiO_2/PDMS foil diffracting a sunlight beam. (c) White light back-illuminated cut-out figure observed through a concave G-SiO_2/PDMS foil showing a symmetric first-order diffraction pattern at the two sides of the direct transmitted light.

appreciable influence on the pattern characteristics. We will come again to this point later in the text.

Further insight into the dynamics of the grooves upon successive bending was gained by keeping curved the G-SiO_2/PDMS foils during SEM observation. The micrographs in Figure 2b taken for the film situated onto the concave side of the foil curved along the *x* or *y* bending axes show that the accumulated compressive stress releases through the formation of wrinkles consisting of a periodic distribution of valleys and ridges. This arrangement of wrinkles is a direct transformation of the parallel groove pattern observed on the flat surfaces, with the wrinkling period and spacing coinciding with those of the initial cracks. By contrast, the normal-view micrographs of the films placed on the convex side (Figure 2c) show the development of similarly spaced big grooves where the gap separating the cracked SiO_2 strips is larger than it is in the flat state. The checkered pattern partially observable in Figure 2b (right) is due to the additional parallel cracking line pattern perpendicular to the bending axis due to previous bending events.

3.2. Switchable Light Diffraction. A remarkable property of the groove structure generated by bending the G-SiO_2/PDMS surfaces is that they work as switchable optical gratings. Figure 4a shows that the flat or bent foil covered with the G-SiO_2 film at the convex side was transparent. By contrast, when the foil is bent with the G-SiO_2 film at the concave side it behaves as a diffraction grating splitting the white light beam into its components. This phenomenon can be observed without using any optical setup. Thus, Figure 4b shows the diffraction pattern of a beam of sunlight traversing the foil when falling on the concave surface. The diffraction performance of this system is further proved in Figure 4c showing the formation of a well-defined symmetric first order spectral image at both sides of an illuminated cut-out figure observed through the concave G-SiO_2/PDMS foil. This transition from a transparent configuration (i.e., flat or convex surface) to a grating configuration was fully reversible and reproducible. The reversibility was tested by repeating the process more than 1000 times with the same foil (see next section).

To understand the origin of these diffraction effects we illuminated two concave surfaces with a 532 nm laser focused in a line oriented either along the *x* or *y* bending axis and measured the distance between the diffraction maxima and the relative intensity of the individual lines. The obtained results are gathered in Figure 5a. The experimental patterns can be directly simulated by assuming a Fraunhofer diffraction by the periodic undulation observed in the concave bent surfaces as shown in Figure 2b (see Supporting Information, S3 for details about the calculations). The optical grating possibilities of the G-SiO_2/PDMS foils are further evidenced in Figure 5b showing the diffraction pattern obtained when the concave surface adopts a hemispherical shape by pressing simultaneously the four corners of the foil. In this case, the laser diffraction pattern is a combination of the single patterns obtained by edge bending along the *x* and *y* axis. A similar pattern was obtained when the foils were bent along an axis other than *x* or *y*. This evidence supports the notion that the *x* and *y* axes are determined by specific directions of the G-SiO_2 film nanostructure and not by the foil manipulation.

Equivalent experiments carried out with G-TiO_2/PDMS foils showed a similar decreasing trend of the crack spacing with the tilting angle (data not shown) than that reported in Figure 3 for the G-SiO_2/PDMS foils. However, in this system with nanocolumnar TiO_2 thin films no significant differences were found by bending along the *x* or *y* axis (see Supporting Information, Figure S4). This different behavior can be related with that intrinsically the TiO_2 nanocolumnar GLAD thin films are in-plane isotropic due to the low tendency of these oxide films to develop bundles of nanocolumns specially at high glancing angles.[17,23] This outcome clearly stresses the

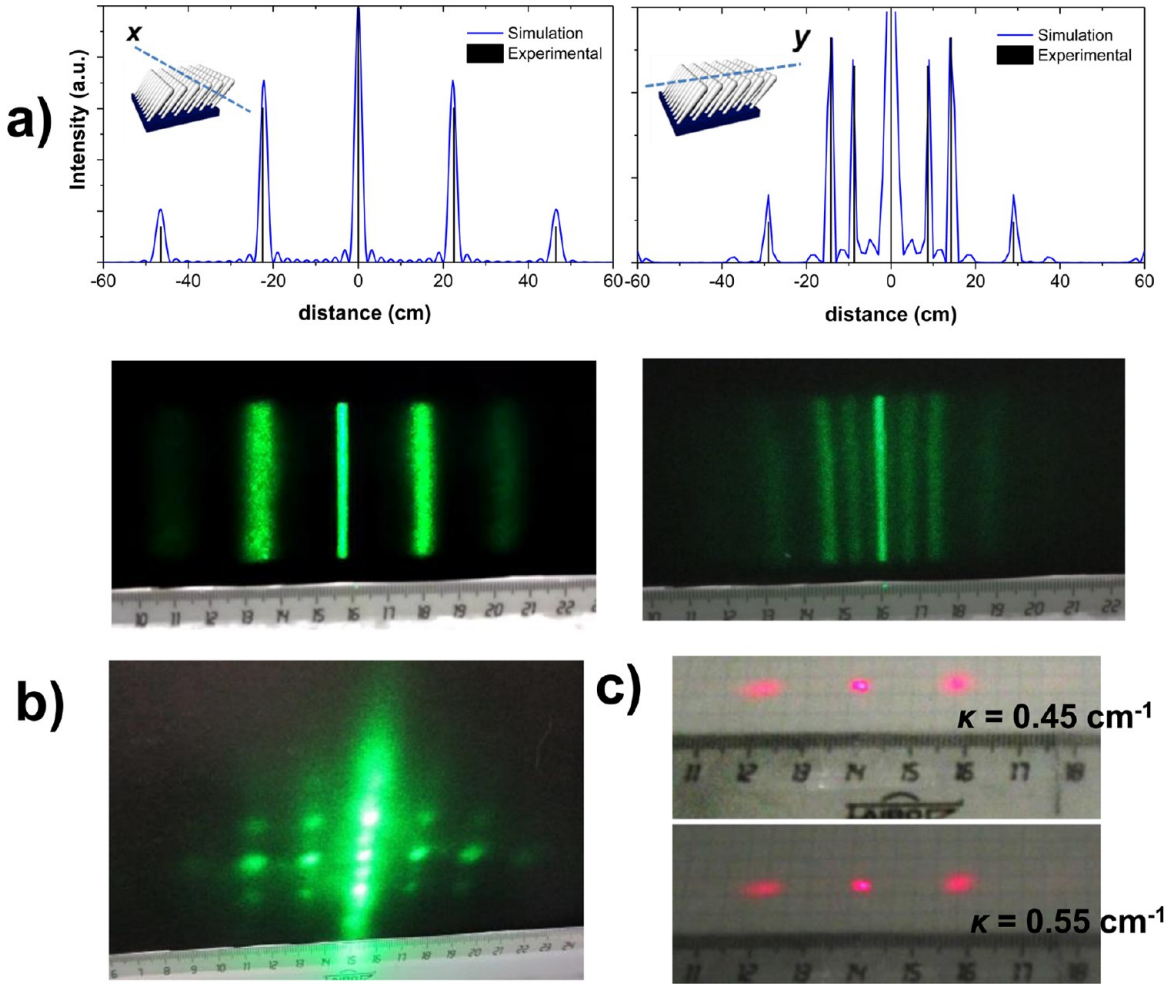

Figure 5. (a) Diffraction patterns corresponding two concave surfaces of the same G-SiO_2/PDMS foil illuminated with a 532 nm laser focused along a line parallel to the *x* and *y* bending axis. The experimental and calculated Fraunhofer diffraction patterns for the two axes are also included in the figure. (b) Diffraction of a 532 nm laser dot by a G-SiO_2/PDMS foil with the oxide film covering the concave hemispherical surface, which is bent by pressing the four corners simultaneously. (c) First-order diffraction pattern of a 635 nm laser measured by changing the curvature of the G-SiO_2/PDMS foil bent along the *x* axis forming a concave surface. All the examples of this figure correspond to a ~300 nm thick G-85°SiO_2/PDMS foil. The distance between the samples and the screen was ~13 cm, and the laser lateral spot size was ~2 mm.

importance of the film nanostructure for the control of the micropatterning processes of PDMS when deposited on its surface.

Another outstanding characteristic of the light diffraction by the concave surfaces was that the diffraction patterns did not depend on the surface curvature but on the deposition angle of the films, and therefore, they were entirely controllable by the manufacturing process. We experimentally determined a minimal curvature of $\kappa = 0.55$ cm^{-1} to observe the light diffraction. At higher curvatures ($\kappa = 0.45$ cm^{-1}) the diffraction pattern remained constant as shown in Figure 5c.

Another remarkable feature of the G-SiO_2/PDMS system is that the average crack spacing is independent of the thin-film thickness. This was proved by verifying that identical micropatterns are obtained for thin films of ~50, 100, 300, and 600 nm when deposited at the same glancing angle. As reported above, in the course of these investigations it was also found that groove spacing was independent of the bending magnitude initially applied to the foil to produce the surface cracking. This behavior contrasts with the reported behavior of wrinkled PDMS surfaces where wrinkling-related diffraction effects are tightly dependent on the thickness of the stiff films coating the PDMS and on the magnitude of the experienced strain.[10−12,30,31] Other studies about cracking of thin films on compliant substrates also reveal that the average intercrack distance is always inversely proportional to the strain.[10,24−26] We attribute the singular behavior of our system to the coupling between the PDMS surface wrinkling processes generally developed by this material to accommodate the bending-induced stress and a tectonic-like behavior of the intercrack G-SiO_2 (or G-TiO_2) regions. The collision behavior of these regions when bending would be determined by the deposited film and yield a specific distribution of valleys and ridges at a given periodicity, which remains invariable at any curvature (Figure 2b). In this model the accommodation of the additional stress induced by increasing the curvature would produce an increase in the height of the ridges but not a modification of the intercrack spacing.

3.3. Fabrication of Optical Patterns. Another remarkable optical effect of the G-SiO_2/PDMS foils usable for invisible labeling applications is the global loss of the foil transparency when they are properly bent. This blurring effect is a direct consequence of the diffraction of light along the whole visible spectrum studied in the previous section. Figure 6a shows how

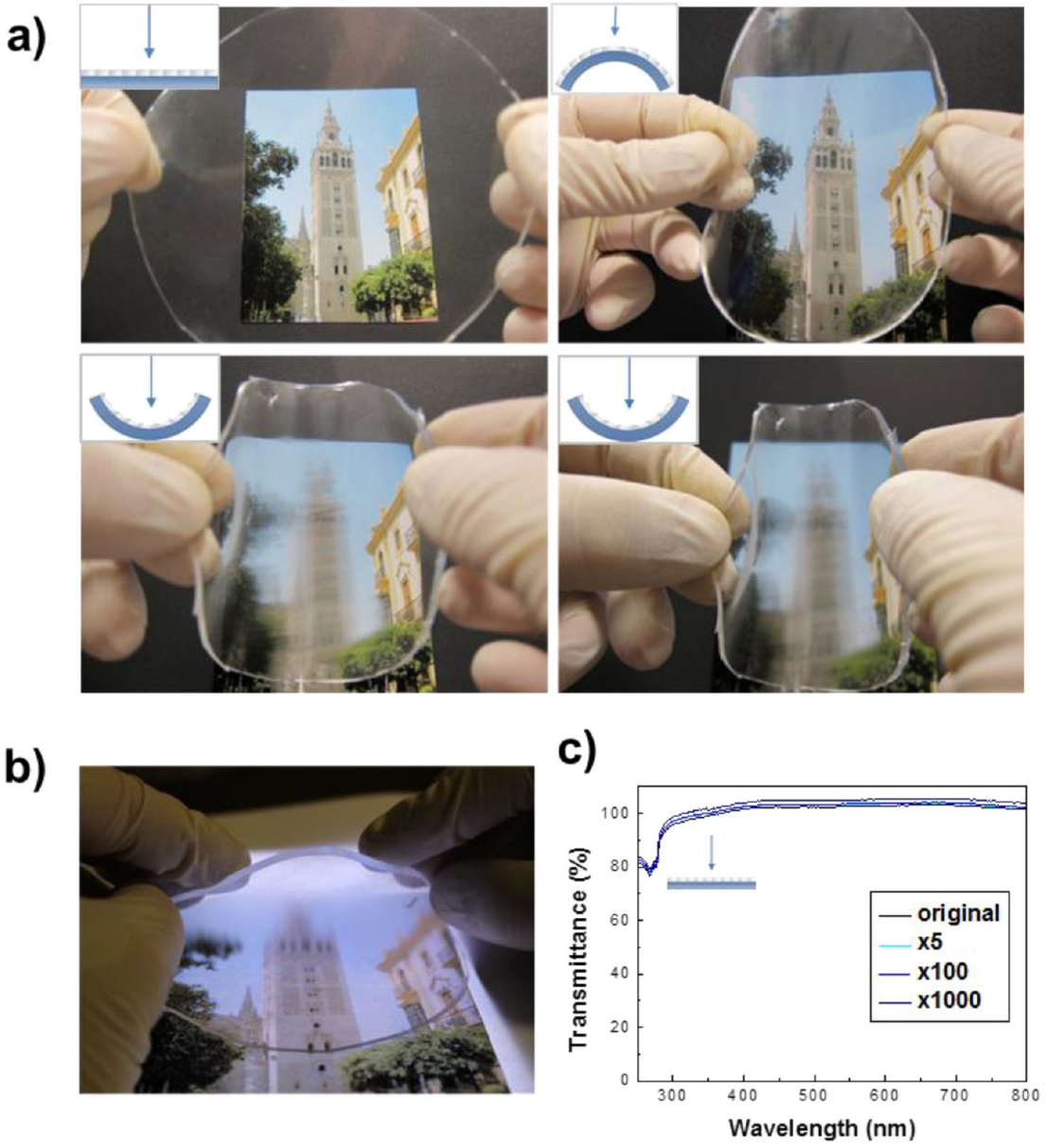

Figure 6. (a) Set of pictures demonstrating the loss of transparency of a G-SiO_2/PDMS concave surface in comparison with the transparency of the coated foil in flat and convex configurations. The examples correspond to a coated ~15 cm diameter PDMS disk. The two bottom pictures are examples of the concave surface with two different curvatures. (b) Picture showing that the loss of transparency is locally restricted to the bent zone, whereas the flat region remains transparent. (c) UV−vis transmission spectra of a SiO_2 thin film bent 5, 100, and 1000 times. All the examples of this figure correspond to a ~300 nm thick SiO_2 film deposited at 85° of glancing angle on a PDMS foil.

a printed image appears blurred when observed thorough a bent foil with the G-SiO_2 film placed at the concave side. Since the regular groove pattern spreads over the entire bent surface, this effect can be observed through relatively large area foils as in the example of the figure. In addition, if only a region of the foil is bent, the flat region remains transparent as shown in Figure 6b. The observed visual loss of transparency was less dependent than the diffraction phenomena on the column microstructure and the specific orientation of the bending axis. This characteristic would facilitate the up-scaling of the process to coat large areas. Thus, large areas would perform similarly with respect to the light blurring even if the local microstructure (tilting angle and density) of the nanocolumnar film could slightly vary from a zone to the other due to slight differences in the glancing angle or the presence of any other inhomogeneity.

It is interesting to stress that the bending-induced light diffraction and the related local blurring process are fully reversible effects. Figure 6c shows that the optical transmission of a G-SiO_2/PDMS in the range of 250−800 nm remained invariable after 1000 bending events, and how in all the cases the coated foils became transparent when they were brought back to their flat state.

A straightforward application of the local optical diffusing effect is the development of invisible labels, that is, motives that are invisible when the film is relaxed and visible by bending. Printed figures or patterns can be easily designed on the surface of PDMS by depositing the nanocolumnar films using shadow masks. An example of this approach is presented in Figure 7

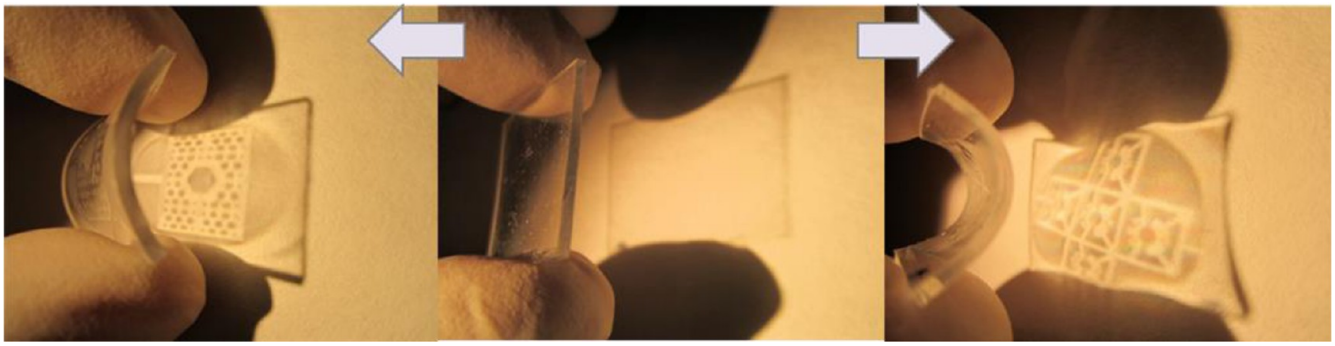

Figure 7. Pictures of a PDMS foil double-side deposited by using two different shadow masks. The projected light reveals the patterns printed onto the concave surface, whereas the pattern in the opposite convex surface is invisible. All the examples of this figure correspond to a ∼300 nm thick SiO_2 film deposited at 85° of glancing angle on a PDMS foil.

where each side of a PDMS foil has been coated with a G-SiO_2 film using different shadow masks. The printed structures can be neatly seen by the naked eye on the surface of the bent foil and also by projecting on a screen with direct white light illumination as shown in the figure. Although the fabrication of patterns formed by local surface wrinkling after deposition or plasma oxidation of PDMS foils through shadow masks has been reported previously,[2,30−32] a clear advantage of our procedure is that it permits to pattern each side of the foil independently. In this way, two different labels can be extracted from a double-side coated foil depending on the side forming a concave surface (Figure 7) when the surface is observed or illuminated. Furthermore, if the deposition of a G-SiO_2 film is carried out onto a curved substrate the structure appears either blurred or transparent when the foil is flat or curved, respectively (data not shown). All these procedures could be used to encrypt information on transparent foils that would be easily retrieved by mechanical actuation with no need of optical set-ups.

4. CONCLUSIONS

In this work we have demonstrated that reversible/switchable gratings can be obtained by bending flexible PDMS foils coated with nanocolumnar SiO_2 thin films prepared by GLAD. The simplicity of the method is proved by the fact that the PDMS foil, coated at room temperature in a single step, can be bent without any special precaution or consideration about the curvature degree (e.g., any unspecific hand bending produces quite reproducible results).

The mechanical stress induced by the first bending event is released by the formation of a regular micrometric parallel crack structure. Once this pattern is formed, the structure can accommodate the stress of subsequent bending events by either increasing the intercrack spacing (i.e, convex surfaces) or by forming a parallel periodic distribution of valleys and crests (i.e., concave surfaces) with a periodicity defined by the intercrack spacing. These regular structures are the diffractive elements responsible of the optical properties of the concave surfaces. Note that the characteristics of the pattern (i.e., intercrack distances and periodicity) are reproducibly determined by the thin-film nanostructure and not by the bending process. In summary, when the film is bent forming a concave surface the PDMS wrinkles, and the oxide film forms a periodic distribution of valleys and ridges following the substrate undulations and preserving the pattern structure.

Two important features of the reported process differ from the common knowledge about patterning based on wrinkling or cracking of films on compliant substrates. The first one is its formation by manual bending instead of by well-controlled uniaxial straining. The second and most important difference is that the magnitude of the externally applied stress (i.e., degree of bending) does not affect the resulting pattern structure, which is entirely dependent on the thin film nanostructure. Besides, the obtained results show that although the pattern generation upon bending is quite dependent on film structural parameters linked to the film nanocolumnar structure (i.e., tilting angle and thin-film density) and its in-plane anisotropy/isotropy, it is independent of its thickness. However, to fully understand this mechanism of bending-induced fracture and why it is determined by the film nanostructure, mechanical simulations are deemed necessary.

Because of the large variety of single and multilayered nanostructured organic, inorganic, and hybrid thin films that can be fabricated by GLAD (i.e., locally anisotropic films, nanostructured multilayers, photonic crystals, etc.) and the extreme simplicity of the procedure we can foresee that the methodology outlined here can be a starting point for new micro/nanopatterning design strategies of photonic elements, optomechanical actuators, reversible microfluidics valves, controlled wetting or security labeling, among others.

■ ASSOCIATED CONTENT

Ⓢ Supporting Information

Figures S1, S2, and S4 and calculation of the diffraction maxima shown in Figure 5 (S3).This material is available free of charge via the Internet at http://pubs.acs.org."

■ AUTHOR INFORMATION

Corresponding Author

*E-mail: angel.barranco@csic.es.

Author Contributions

The manuscript was written through contributions of all authors. All authors have given approval to the final version of the manuscript.

Notes

The authors declare no competing financial interest.

■ ACKNOWLEDGMENTS

We thank the Junta de Andalucía (TEP8067, FQM-6900 and P12-FQM-2265) and the Spanish Ministry of Economy and Competitiveness (Projects CONSOLIDER-CSD 2008-00023,

MAT2013-40852-R and RECUPERA 2020) for financial support.

REFERENCES

(1) Bowden, N.; Brittain, S.; Evans, A. G.; Hutchinson, J. W.; Whitesides, G. M. Spontaneous Formation of Ordered Structures in Thin Films of Metals Supported on an Elastomeric Polymer. *Nature* **1998**, *393*, 146−149.

(2) Bowden, N.; Huck, W. T. S.; Paul, K. E.; Whitesides, G. M. The Controlled Formation of Ordered, Sinusoidal Structures by Plasma Oxidation of an Elastomeric Polymer. *Appl. Phys. Lett.* **1998**, *75*, 2557−2559.

(3) Huck, W. T. S.; Bowden, N.; Onck, P.; Pardoen, T.; Hutchinson, J. W.; Whitesides, G. M. Ordering of Spontaneously Formed Buckles on Planar Surfaces. *Langmuir* **2000**, *16*, 3497−3501.

(4) Ohzono, T.; Monobe, H.; Shiokawa, K.; Fujiwara, M.; Shimizua, Y. Shaping Liquid on a Micrometre Scale Using Microwrinkles as Deformable Open Channel Capillaries. *Soft Matter* **2009**, *5*, 4658−4664.

(5) Khare, K.; Zhou, J.; Yang, S. Tunable Open-Channel Microfluidics on Soft Poly(dimethylsiloxane) (PDMS) substrates with sinusoidal grooves. *Langmuir* **2009**, *25*, 12794−12799.

(6) Efimenko, K.; Rackaitis, M.; Manias, E.; Vaziri, A.; Mahadevan, L.; Genzer, J. Nested Self-Similar Wrinkling Patterns in Skins. *Nat. Mater.* **2005**, *4*, 293−297.

(7) Jiang, X.; Takayama, S.; Qian, X.; Ostuni, E.; Wu, H.; Bowden, N.; LeDuc, P.; Ingber, D. E.; Whitesides, G. M. Controlling Mammalian Cell Spreading and Cytoskeletal Arrangement with Conveniently Fabricated Continuous Wavy Features on Poly(dimethylsiloxane). *Langmuir* **2002**, *18*, 3273−3280.

(8) Tawfick, S.; De Volder, M.; Davor, C.; Park, S. J.; Oliver, C. R.; Polsen, E. S.; Roberts, M. J.; Hart, A. J. Engineering of Micro- and Nanostructured Surfaces with Anisotropic Geometries and Properties. *Adv. Mater.* **2012**, *24*, 1628−1674.

(9) Maruyama, T.; Hirakata, H.; Yonezu, A.; Minoshima, K. Realization of Freestanding Wrinkled Thin Films with Flexible Deformability. *Appl. Phys. Lett.* **2011**, *98*, 041908.

(10) Stafford, C. M.; Harrison, C.; Beers, K. L.; Karim, A.; Amis, E. J.; Vanlandingham, M. R.; Kim, H. C.; Volksen, W.; Miller, R. D.; Simonyl, E. E. A Buckling-Based Metrology for Measuring the Elastic Moduli of Polymeric Thin Films. *Nat. Mater.* **2004**, *3*, 545−550.

(11) Genzer, J.; Groenewold, J. Soft Matter with Hard Skin: From Skin Wrinkles to Templating and Material Characterization. *Soft. Mater.* **2006**, *2*, 310−323.

(12) Chung, J. Y.; Nolte, A. J.; Stafford, C. Surface Wrinkling: A Versatile Platform for Measuring Thin-Film Properties. *Adv. Mater.* **2011**, *23*, 349−368.

(13) Chung, J. Y.; Chastek, T. Q.; Fasolka, M. J.; Ro, H. W.; Stafford, C. M. Quantifying Residual Stress in Nanoscale Thin Polymer Films via Surface Wrinkling. *ACS Nano* **2009**, *3*, 844−852.

(14) Robbie, K.; Brett, M. J. Sculptured Thin Films and Glancing Angle Deposition: Growth Mechanics and Applications. *J. Vac. Sci. Technol.* **1997**, *15*, 1460−1465.

(15) Hawkeye, M. M.; Brett, M. J. Glancing Angle Deposition: Fabrication, Properties, and Applications of Micro- and Nanostructured Thin Films. *J. Vac. Sci. Technol., A* **2007**, *25*, 1317−1335.

(16) Kennedy, S. R.; Brett, M. J. Porous Broadband Antireflection Coating by Glancing Angle Deposition. *Appl. Opt.* **2003**, *42*, 4573−4579.

(17) Gonzalez-García, L.; Barranco, A.; Paez, A. M.; Gonzalez-Elipe, A. R.; García-Gutierrez, M. C.; Hernández, J. J.; Rueda, D. R.; Ezquerra, T. A.; Babonneau, D. Structure of Glancing Incidence Deposited TiO_2 Thin Films as Revealed by Grazing Incidence Small-Angle X-ray Scattering. *ChemPhysChem* **2010**, *11*, 2205−2208.

(18) Sanchez-Valencia, J. R.; Toudert, J.; Borras, A.; Lopez-Santos, C.; Barranco, A.; Feliu, I. O.; Gonzalez-Elipe, A. R. Tunable In-Plane Optical Anisotropy of Ag Nanoparticles Deposited by DC Sputtering onto SiO_2 Nanocolumnar Films. *Plasmonics* **2010**, *5*, 241−250.

(19) Van Kranenburg, H.; Lodder, C. Tailoring Growth and Local Composition by Oblique-Incidence Deposition: a Review and New Experimental Data. *Mater. Sci. Eng., R* **1994**, *11*, 295−354.

(20) Sanchez-Valencia, J. R.; Toudert, J.; Borras, A.; Barranco, A.; Lahoz, R.; de la Fuente, G. F.; Frutos, F.; Gonzalez-Elipe, A. R. Selective Dichroic Patterning by Nanosecond Laser Treatment of Ag Nanostripes. *Adv. Mater.* **2011**, *23*, 848−853.

(21) Gonzalez-Garcia, L.; Parra-Barranco, J.; Sanchez-Valencia, J. R.; Ferrer, J.; Garcia-Gutierrez, M. C.; Barranco, A.; Gonzalez-Elipe, A. R. Tuning Dichroic Plasmon Resonance Modes of Gold Nanoparticles in Optical Thin Films. *Adv. Funct. Mater.* **2013**, *23*, 1655−1663.

(22) Sanchez-Valencia, J. R.; Blaszczyk-Lezak, I.; Espinos, J. P.; Hamad, S.; Gonzalez-Elipe, A. R.; Barranco, A. Incorporation and Thermal Evolution of Rhodamine 6G Dye Molecules Adsorbed in Porous Columnar Optical SiO_2 Thin Films. *Langmuir* **2009**, *25*, 9140−9148.

(23) Gaillard, Y.; Rico, V. J.; Jimenez-Pique, E.; González-Elipe, A. R. Nanoindentation of TiO_2 Thin Films with Different Microstructures. *J. Phys. D: Appl. Phys.* **2009**, *42* (145305), 1−9.

(24) Thouless, M. D. Crack Spacing in Brittle Films on Elastic Substrates. *J. Am. Ceram. Soc.* **1990**, *73*, 2144−2146.

(25) Thouless, M. D.; Li, Z.; Douville, N. J.; Takayama, S. Periodic Cracking of Films Supported on Compliant Substrates. *J. Mech. Phys. Solids* **2011**, *59*, 1927−1937.

(26) Zhu, X.; Mills, K. L.; Peters, P. R.; Bahng, J. H.; Liu, E. H.; Shim, J.; Naruse, K.; Csete, M. E.; Thouless, M. D.; Takayama, S. Fabrication of Reconfigurable Protein Matrices by Cracking. *Nat. Mater.* **2005**, *4*, 403−406.

(27) Huh, D.; Mills, K. L.; Zhu, X.; Burns, M. A.; Thouless, M. D.; Sakayama, S. Tunable Elastomeric Nanochannels for Nanofluidic Manipulation. *Nat. Mater.* **2007**, *6*, 424−428.

(28) Alcaire, M.; Sanchez-Valencia, J. R.; Aparicio, F. J.; Sagui, Z.; Gonzalez-Gonzalez, J. C.; Barranco, A.; Oulad-Zian, Y.; Gonzalez-Elipe, A. R.; Midgley, P.; Espinos, J. P.; Groening, P.; Borras, A. Soft plasma Processing of Organic Nanowires: A Route for the Fabrication of 1D Organic Heterostructures and the Template Synthesis of Inorganic 1D Nanostructures. *Nanoscale* **2011**, *3*, 4554−4559.

(29) Barranco, A.; Cotrino, J.; Yubero, F.; Espinos, J. P.; Gonzalez-Elipe, A. R. Synthesis of SiO_2 and $SiO_xC_yH_z$ Thin Films by Microwave Plasma CVD. *Thin Solid Films* **2001**, *401*, 150−158.

(30) Chua, D. B. H.; Ng, H. T.; Li, S. F. Y. Spontaneous Formation of Complex and Orderer Structures on Oxygen-Plasma-Treated Elastomeric Polydimethylsiloxane. *Appl. Phys. Lett.* **2000**, *76*, 721−723.

(31) Kim, P.; Hu, Y.; Alvarenga, J.; Kolle, M.; Suo, Z.; Aizenberg, J. Tunable Optical Diffuser Based on Deformable Wrinkles Rational Design of Mechano-Responsive Optical Materials by Fine Tuning the Evolution of Strain-Dependent Wrinkling Patterns. *Adv. Opt. Mater.* **2013**, *1*, 381−388.

(32) Ohzono, T.; Suzuki, K.; Yamaguchi, T.; Fukuda, N. Tunable Optical Diffuser Based on Deformable Wrinkles. *Adv. Opt. Mater.* **2013**, *1*, 374−380.